American Journal of Chemistry 2016, 6(2): 36-46
DOI: 10.5923/j.chemistry.20160602.03

The Influence of Addition of CdS on the Properties of TiO_2 Nanoparticle Prepared by Sol-Gel Method

Ramzei R. AL-Ani, Yousif K. Abdul Amir, Fadhela M. Hussein*

Chemistry Department, College of Science, AL-Mustansiriyah University, Baghdad, Iraq

Abstract In this study TiO_2/CdS nanoparticles synthesized through chemical reaction by sol-gel method. The nanoparticles were characterized using techniques like X-ray diffraction (XRD), scanning electron microscope (SEM), UV-visible reduction spectroscopy and atomic force microscope AFM. TiO_2/CdS Nanoparticles, the coupling of CdS nanoparticles with TiO_2 resulted in changes in electronic absorption and crystal shape. Spectral techniques used to measured particle sized, which was found around (17.42) nm. SEM image shows that the TiO_2/CdS are spherical in shape with average diameter (28.5) nm, the photo degradation of p-nitrotolune was observed by kinetic studies indicate that the reaction to pseudo first order and decreasing of rate reaction with increasing initial concentration for p-nitrotolune.

Keywords Sol-Gel method, Nano TiO_2/ CdS, Photocatalytic activity

1. Introduction

Nano technology has remained tiny exciting field of interest of research and gained a great importance from the past two decades. Nanoparticles are smaller microscopic particles or nano-technology allows us to address the matter at the molecular level (much less than 100nm) [1].

Attracted semiconducting nanoparticles to the benefits over the past decade due to the unique size of its kind attached, chemical and physical properties. [2]

Semiconducting nanoparticles due to specific optical, electronic and catalytic properties, and damping is achieved mostly bonds capping such bipyridine thiolates have been reported to minimize surface defects and increase luminescence efficiency. [3]

Nano-sized particles of semiconductor material has gained more attention in recent years due to the characteristics of the coveted and their applications in various fields such as catalysts, prospector, optical devices, Nanomaterials. This highly functional contains the electronic and structural properties, and new thermal involving the interests of scientific and high in basic and applied fields. [4]

Light heterogeneous is one of the advanced oxidation processes for the removal of organic contaminants.

In this process, metal oxide semiconductors absorb light and generate an activity which leads to complete oxidation of organic compounds found in wastewater. TiO_2 metal oxide semiconductor with a wide band gap (3.2ev). And the role of transition metal ions in TiO_2 is that the transition metal ion provides a way to trap charge carriers and thus improve the efficiency of the catalyst. [5]

The main goal of the dope is to make a bathochromic turns into a low band gap, or the forefront of countries within the band gap, which causes the absorption of light more clearly.

It seems that modifying the surface of nanoparticles TiO_2 be more beneficial than modifying TiO_2 wholesale.

Photocatalysts semiconductor alongside the exhibition is very high optical activity of both gas and liquid phase reactions by increasing the separation of the charge and the expansion of the scope of the power of excitement image.

The molecular geometry, surface texture and size of the particles play an important role in the transfer. There particle electron great deal of interest in coupling particales semiconductors with various TiO_2, with couples like TiO_2 -Bi_2S_3, TiO_2-WO_3, TiO_2-SnO_2, TiO_2-MoO_3, and iO_2-Fe_2O_3 [6].

Here in TiO_2/CdS were prepared by sol- gel method. Its photocatalytic activity was evaluated by degradation of p-nitrotolune and effects of various parameters on the photocatalytic of TiO_2 /CdS were studied.

2. Materials and Methods

Cadmium chloride, sodium sulfide (Merck) and Titanium tetraisopropoxide was supplied by Sigma-Aldrich with purity of 97%. thioglycerol (Fluka). All reagents consumed were of analytical grade purity and were procured from Merck chemical Reagent Co. LTD. Technical grade (Sigma, Aldrich), ethanol absolute (Merck) and distilled water used for the preparation of nanoparticles by the sol-gel. p-nitrotolune was supplied by Sigma-Aldrich with purity of

* Corresponding author:
fadhussein_99@yahoo.com (Fadhela M. Hussein)
Published online at http://journal.sapub.org/chemistry

99.5%.

The prepared crystalline nanoparticles structure were characterized using X-ray diffraction (Shimadzu XRD -6000) at room temperature operating at 40 Kv, current 30 mA range (20-80) deg speed 5(deg/min), preset time =0.6 sec. Using CuKα, λ = 0.15406 nm radiation.

Surface morphology was studied by using SEM (Sigma). electronic spectra UV-visible spectrophotometer (100 Conc/ Varian. USA), the average particale size were measured using atomic force microscope (AFM) AA300 scanning probe microscope angstrom Advanced Inc.

The surface area of nanoparticles was studied by using Instrument NOVA station A.

Fourier transform infrared (FT-IR) measurements were executed using perkin Elmer spectrum, the recording spectrum in the range (400-4000 cm^{-1}). The U.V light is generated from a 150 w medium pressure mercury lamp supplier from PHYWE (England).

The photocatalytic activity of the calcined powder was investigated by the degradation of p-nitrotolune solution was employed as model pollutant to measure the photocatalytic activity of TiO_2/ CdS catalysts.

40 ml of p-nitrotolune aqueous solution, the solution was placed in a photocatalytic reactor and stirred and irradiated with UV-lamp, 3 ml of the suspension was extracted and separate the powder from the supernatant for 15 min by centrifuged at 7000 rev/min .UV-Visible spectroscopy was used to generate time dependent absorbance changes in the range 200-800 nm .degraded of p- nitrotolune solution was determined by measuring the absorbance at λ = 285 nm.

Synthesis of TiO_2 coupled CdS nanoparticle.

(A) The synthesis of TiO_2 was obtained from titanium tetra isopropoxide (TTIP) was dissolved in absolute ethanol and deionization water of a molar ratio of Ti:H_2O = 1:4, Nitric acid was used to adjust the pH and for restrain the hydrolysis process of the solution. After for 24 hour the gels were dried under 80°C for 2 hours to evaporate water and organic material to the maximum extent. Then the dry gel was calcination at 450°C for 2 hours were subsequently carried out to obtain desired TiO_2 nanoparticles. [7, 8]

(B) Synthesis of TiO_2/ CdS by addition aqueous solution of step (A) (0.8 gm) dissolved in absolute ethanol with $CdCl_2$ in deionization water molar ratio (2:1), thioglycerol (TG) was added drop wise into the aqueous solution and (0.1 mol) of Na_2S solution was injected drop by drop into the above solution for 60 minute under stirring. Final mixture was stirred for six hours at 70°C reflux. The solid were separated from solution by centrifuge (3500 rpm) for 15 minutes and was washed several times with acetone to get rid of unreacted solvent pale yellow, drying for 4 hours and aging for 72 hour nanoparticle was collect as white.

3. Results and Discussion

X-ray diffraction patterns of TiO_2/CdS by sol-gel technique figure (1) shows peaks at 2 θ = 25.21, 47.95 and 53.82° which belong to (101), (002) and (105) these peaks can be indexed to anatase phase (JCPDS card No.21-1272), and these peaks also appeared in all doped which indicates that CdS doping did not change TiO_2 lattice structure with lower CdS doping exhibited strong preferential orientation of (101) plane.

In the presence of low CdS doping also produced additional small peaks at 2 θ = 27.34, 36.88, 54.92, 63.17 and 68.79 that belong to (002), (102), (004), (104) and (210) related to CdS. The presence of small peaks indicate the formation of new crystallization representing each of the properties TiO_2 and CdS, particle size has been calculated by using the Scherer formula [9]

$$D=0.89\,\lambda/\,B\cos\theta \qquad (1)$$

λ Where is the wave length of X-ray diffraction, B is FWHM in radians of the XRD peak θ and is the angle of diffraction. The particle size of the samples was calculated from eq. (1) Is found equal 17.242 nm.

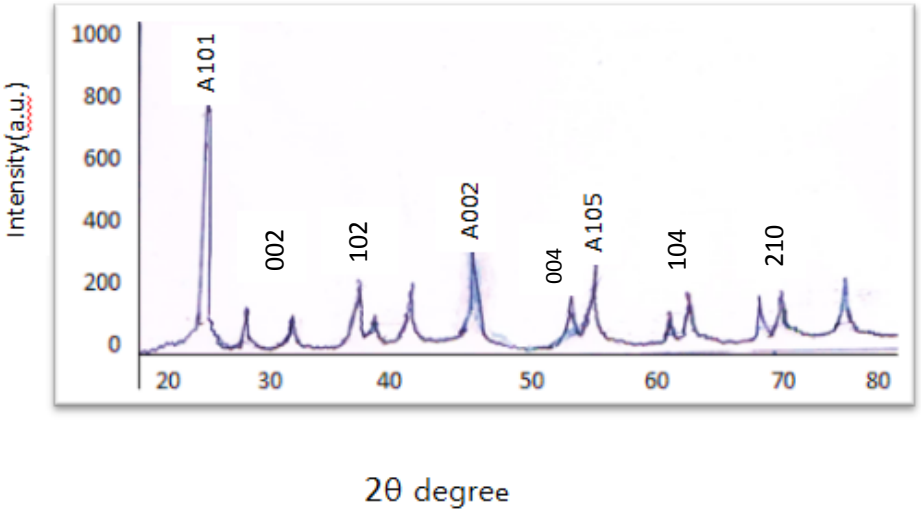

Figure (1). XRD pattern of TiO_2 /CdS nanoparticles by sol-gel method

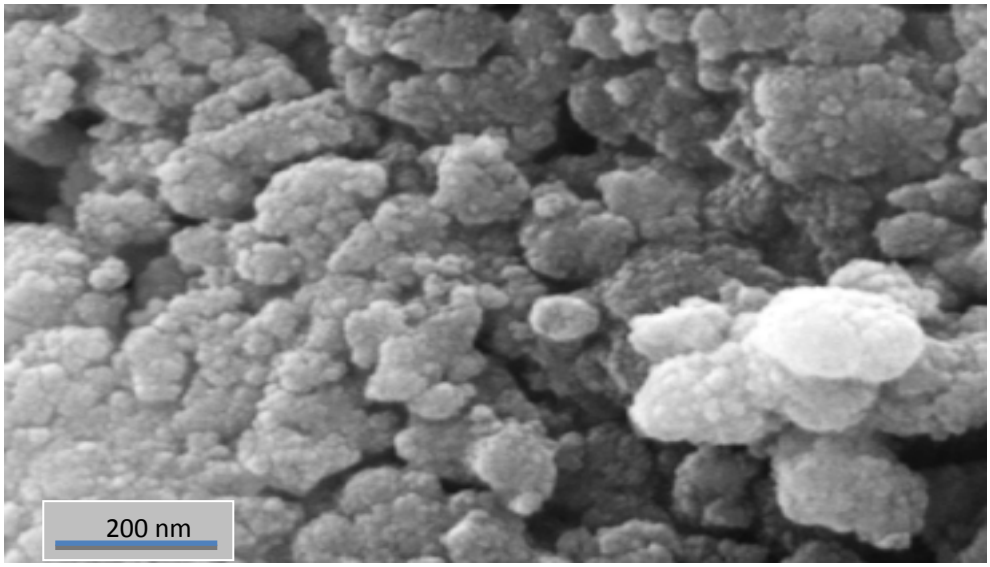

Figure (2). SEM images of TiO_2/CdS nanoparticles

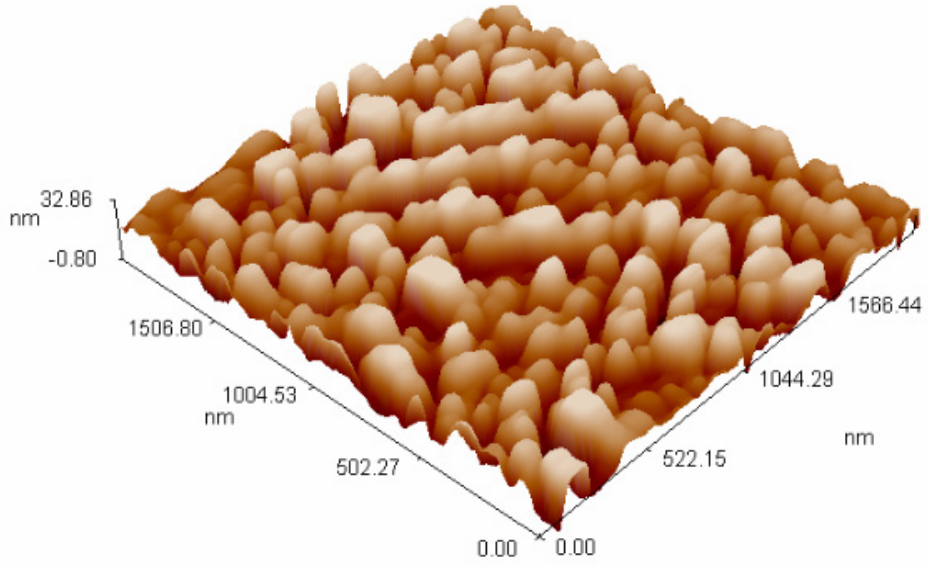

Figure (3). AFM image of TiO_2 coupled CdS nanoparticles

The SEM image derived TiO_2/ CdS nanoparticle of observed in figure (2). This shows average diameter of TiO_2 /CdS nanoparticle is approximately equal 42 nm, the particles agglomerated resulting in increased crystallite size.

However the size of Chrystelle were in the same range as those that show homogenous distribution of CdS nanoparticle coupled TiO_2 nanoparticle by addition the dopant led to crystallite growth.

While Vijayalakshmi et al [8] observed the crystallite size for nano TiO_2 the prepared by hydrothermal method and sol-gel method, TiO_2 nanostructures has grain size of 30 nm by sol- gel method and 100 nm by hydrothermal method.

Figure (3) shows **the AFM** images and corresponding size distributions of TiO_2 coupled CdS nanoparticles. From figure are spherical in shape having average diameter of (76.86 nm) are observed over the entire surface.

The 3D AFM image of material nanopartical in which the regular and distributed CdS on TiO_2 nanoparticles the entire surface can be seen with root-mean –square (RMS) of (3. 09 nm).

Figure (4) represents the **FTIR spectra** of sol-gel derived CdS nanoparticle, strong the band at 3543 cm^{-1} and 1643.41 cm^{-1} in spectra are due to the stretching and bending vibration of the (O-H) group. The medium strong band at 877and 675 cm^{-1} has been assigned as Cd-S band. Figure (5) shows the FTIR spectrum of sol-gel derived from TiO_2 /CdS nanoparticles a band of 2390 cm^{-1} in the spectra is due to the stretching vibration of (S-H) group and the band 1653.05 cm^{-1} is assigned to (O-H) group of absorbed water on the surface of TiO_2/CdS nanoparticle, and the weak bands at 1128.39 cm^{-1} show stretching vibration and 717 cm^{-1} bending vibration of (S-O), the bands 840 $cm^{-1}$and 690 cm^{-1} in the spectra are due to (Cd-S) while strong of band 630.74 and 609 cm^{-1} have been assigned as(Ti-O) bond.

That the results agreement with the result Y.Bar et al [10] and Barman have reported infrared spectra CdS crystalline doped poly vinyl (PVA) the strong band at 679 cm^{-1} and 813 cm^{-1} have been as (Cd-S) band, Concluded that CdS nanoparticle has been synthesis by chemical growth techniques there was no change is the band positions of matrix with doping of CdS in the poly vinyl network [11].

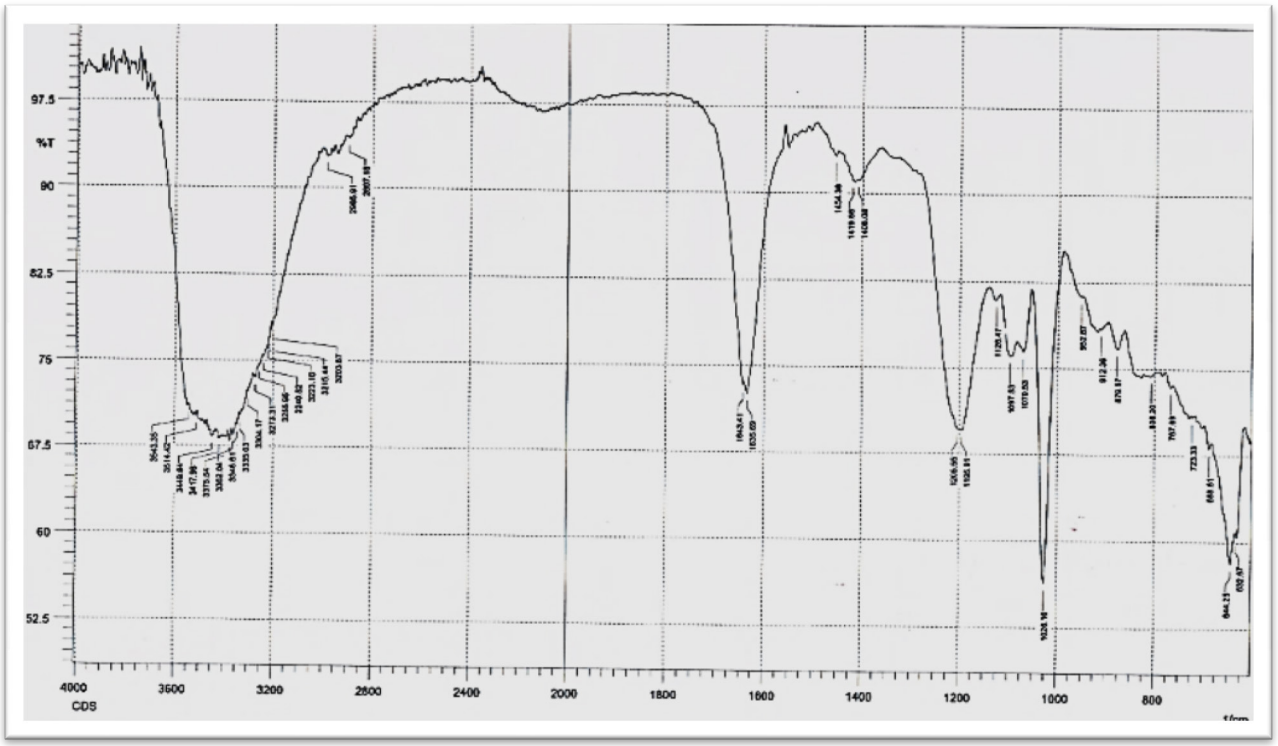

Figure (4). FTIR Spectrum of CdS nanoparticles

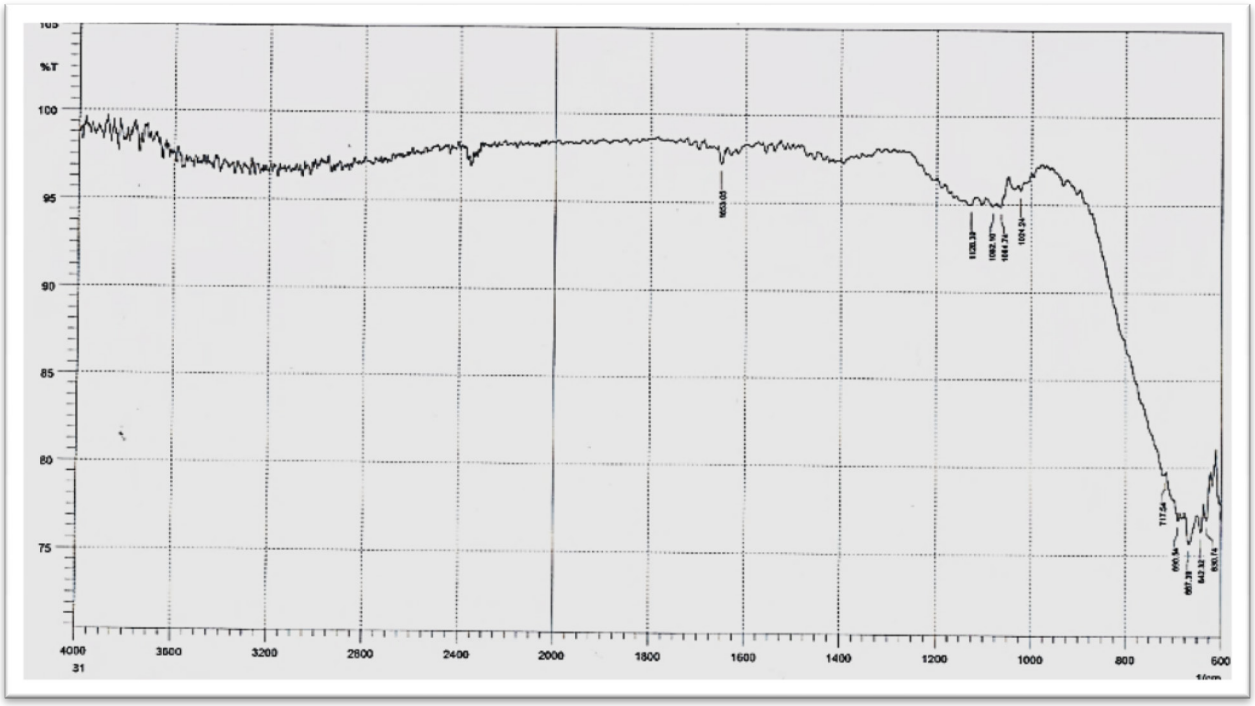

Figure (5). FTIR Spectrum of TiO_2/ CdS nanoparticles

In present work band gap for TiO_2 coupled CdS is calculated using the Tauc relation [12]. Tauc relation is described as

$$(\alpha hv)^{1/n} = A(hv-Eg) \quad (2)$$

Where α is absorption coefficient, A is constant and Eg is the band gap of the materials and exponent (n) that depends on the kind of transition, to locate the possible transition $(\alpha hv)^2$ vs hv is plotted and congruent band gap were obtained from extrapolating the honest portion of the graph on hv axis as shown in the figure (6) the band gap value of TiO_2 /CdS nanoparticale is found to be (3.1 eV), this value is shifted compared with the bulk CdS value and reduce for TiO_2.

The significant red- shift lower band energy of TiO_2 coupled CdS nanoparticle compared to TiO_2 due to coupled effects on the structural and textural parameters of TiO_2.

The valence band energy in TiO_2 /CdS nanoparticle needs lower energy to be excited than that required for that band in TiO_2 pure, this means that the introduction of CdS into TiO_2 should improve its photocatalytic efficiency.

Thus the BET surface area of CdS coupled TiO_2 nanoparticle was (18.69 $m^2.g^{-1}$), the reason is believed to that CdS concentrated a blocked into the pore of nanoparticle and assumption pore geometry typically cylindrical pore geometry will determine how wall surface area is calculated from pore volume [13]. The shape of isotherm is cylindrical pores.

However total pore volume calculated from total volume adsorbed that those collect isotherm data to pressure near saturation to assure all pores are filled and assumed that gas volume adsorbed on free surface is insignificant compared to volume adsorbed in pores.

The isotherms are type IV, which is characteristic of mesoporous materials, figures (7) show the shape of hysteresis loop has often been identified with specific pore structures. The TiO_2 /CdS support exhibit HI type of hysteresis are correspond of H type isotherms according to IUPAC classification [14].

The BET surface area for TiO_2 coupled CdS, table (1) shows of surface area and pore volume of TiO_2 coupled CdS.

Kinetic study of TiO_2 coupled CdS

3.1. Effect Concentration of TiO_2/CdS Nanoparticle

Numerous forms of TiO_2 have been synthesized by different methods with the aim to achieve materials exhibiting desirable physical properties, activity and stability for photocatalytic application [15].

To optimum of catalyst loading was studied within the range of 0.025 to 0.25 gm/l.

Figure (8) shows that photodegradation of p-NT increased gradually with loading of TiO_2 / CdS nanoparticles up to 0.125 gm/l and 66.8% efficiency was achieved after 180 min irradiation time.

When the loading TiO_2 /CdS nanoparticles is lower than optimal the free $OH^{\cdot}$ and $O_2^{\cdot-}$ superoxide radicals generated is proportionally decreases , and if more than optimal due to the scattering of light by excess of nanoparticles was occurred.

As light become hardly to reaches all particles due to agglomeration of particles which reduce the degradation rate [16].

That results similar to the result Muneer et al studied effect of loading on TiO_2 nanoparticle activity for 2- chlorophenol was the optimal catalyst loading (0.2 gm/l) (16).

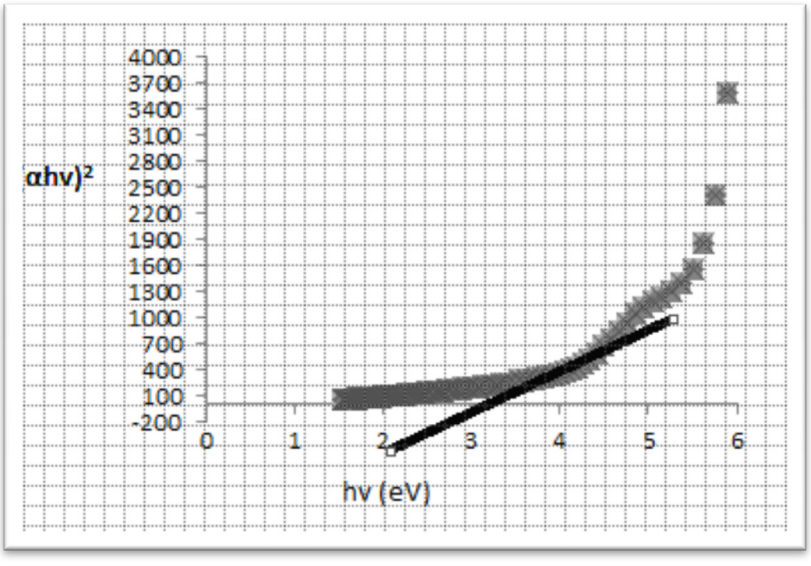

Figure (6). Band gap measurement by plot $(\alpha hv)^2$ via hv for TiO_2/ CdS

Table (1). The surface area and pore volume of sample

Sample	BET S.A ($m^2.g^{-1}$)	BJH average pore diameter (4V/A)A°	Pore diameter (A°)	Pore volume ($cm^3.g^{-1}$)	Total pore volume ($cm^3.g^{-1}$)
TiO_2/ CdS	18.69	132.7	11.88	0.06167	0.05956

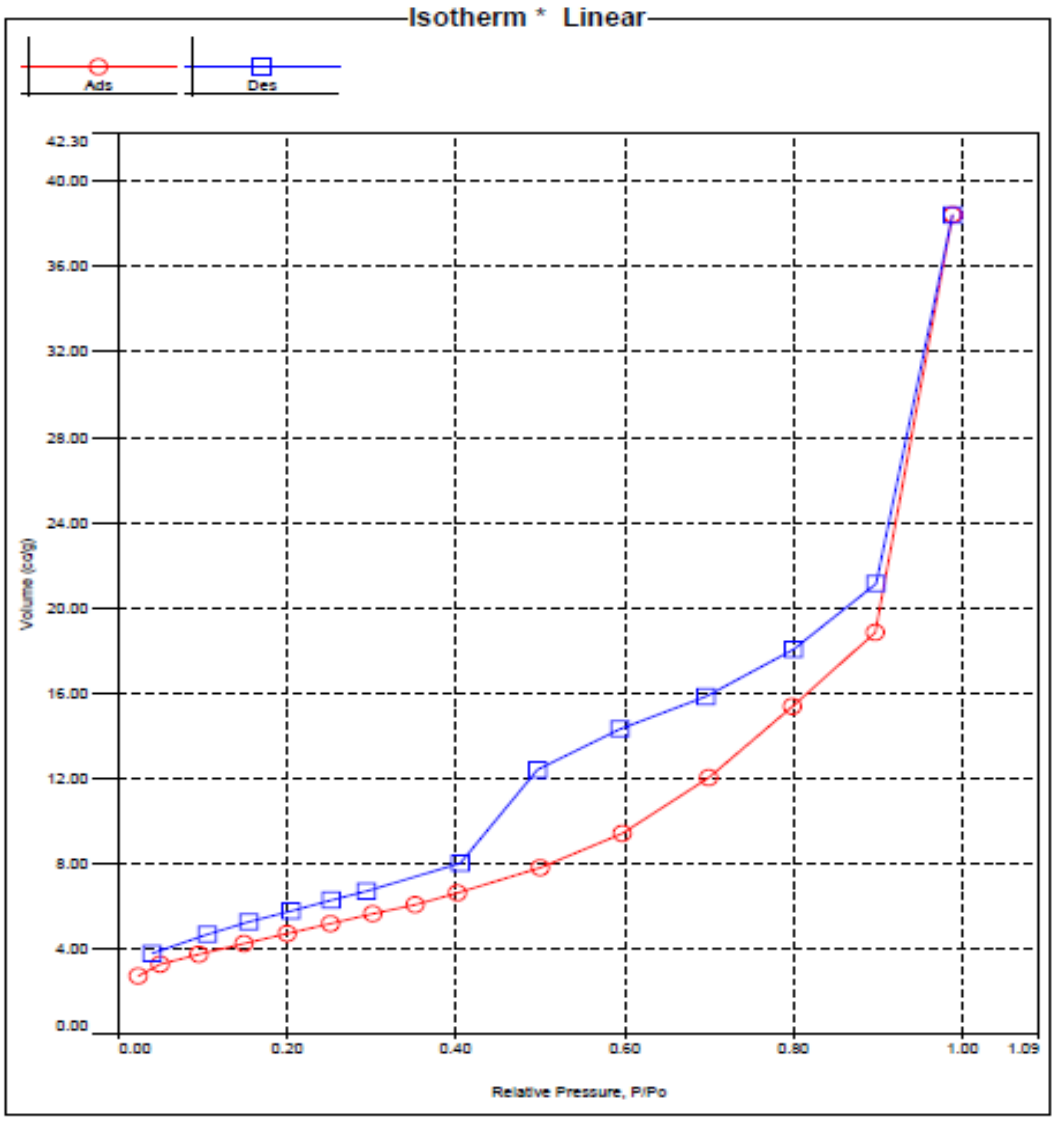

Figure (7). Isotherm of TiO_2/ CdS

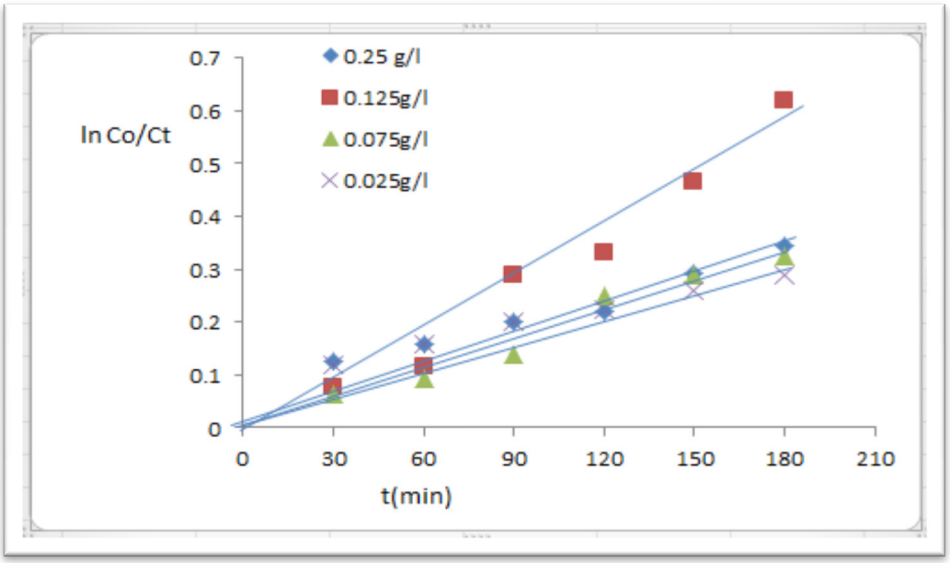

Figure (8). Concentration different of nanoparticle TiO_2/ CdS, p-NT ($1*10^{-4}$)M

3.2. Effect of Initial Concentration of p-NT

The effect of varying 4-NT concentration at range ($1\text{-}7*10^{-4}$M) on its degradation rate is shown in figure (9) from the results of the higher of 4-NT concentration, the higher the degradation efficiency of 4-NT decomposition.

A Langmuir –Hinshelwood medal of relationship can be used to describe the effect of 4-NT concentration on its degradation.

The results clearly that the photocatalytic process is promising of the pollutant, this is occurs for heterogeneous catalytic systems.

When the initial concentration of 4-NT is $7*10^{-4}$ M as presented in figure (9) can be higher efficiency degradation (71.3%) within the 180 min irradiation time.

This observation more molecules are adsorbed as multilayer of molecules on the surface of TiO_2 /CdS nanoparticle which was to contact the photogenerated holes or radicles to lead number of radicles available for attacking the 4-NT.

The concentration of organic substrates in time is also dependent on photonic efficiency during photocatalytic oxidation. [17]

The lower concentration of 4-NT on its degradation the limitation of surface sites for the reaction may control 4-NT decomposition, therefore less the efficiency degradation because decrease photonic efficiency.

A Langmiur – Hinshelwood (L-H) kinetics model, which is commonly expressed as equation (3)

$$1/\ r = 1/k + 1/\ kKC_o \qquad (3)$$

Where k is the reaction rate constant, K is the equilibrium adsorption constant and C_o is the initial concentration.

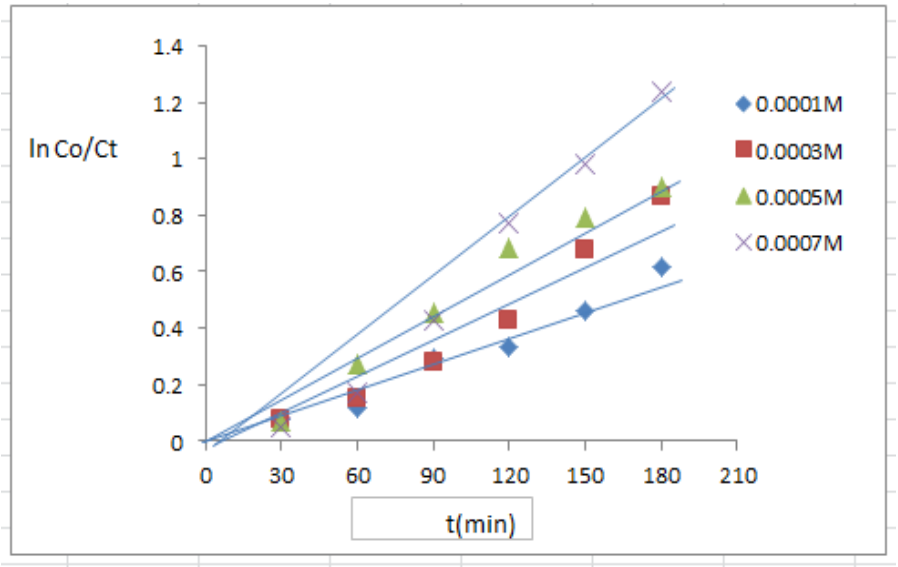

Figure (9). Different concentration of p-NT, TiO_2/CdS nanoparticle (0.125 g/l) pH 5.9, T 25°C

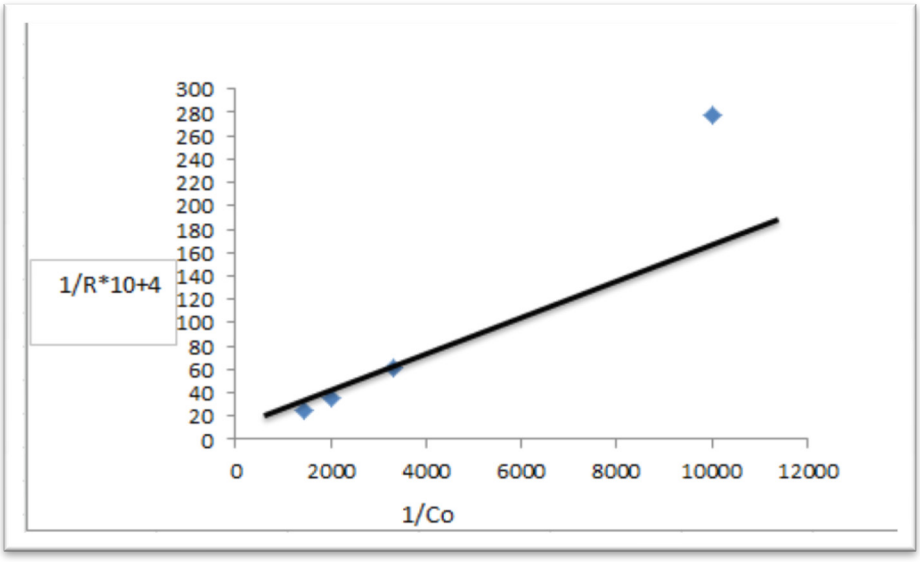

Figure (10). plot of the reverse of the initial rate of p-NT in TiO_2/ CdS nanoparticle (0.125 g/l) against the revese of the initial p- N.T concentration

According to the langmiur –Hinshelwood (L-H) kinetic formula fitted figure (10) a straight line was obtained with an intercept of 1/k and 1/kK from which k and K were estimate at ($0.2 *10^{-4} M^{-1} min^{-1}$) and ($163.398 M^{-1}$).

The high value of adsorption constant (K) indicates that electron density of aromatic ring in 4-NT molecule leads to a stronger adsorption on the (Ti^{+4}) sites at the TiO_2/CdS surface.

Thus the photodegradation of aromatics depends on the substituent group. It is reported that the degradation of chlorodazone by used Au/TiO_2 nanoparticle about one hour irradiation UV-lamp for 30 min the degradation of chlorodazone about 50% could be explained of aromatic rings as well as nature of substituent on the rang like electron donating or electron withdrawing groups which the effect of degradation rate. [18]

3.3. Effect of pH Value

The pH of the solution has strong effect on the photodegradation process, the pH value of 4-NT solution has significant influence on the photocatalytic activity of sample.

The optimal pH of reaction mixture for the photodegradation of 4- NT a series of experiments was conducted at different pH values of (3, 5.9, 7 and 9).

The results increase in pH of 4-NT solution from (3 to 7) led to the enhanced efficiency in the photodegradation of solution, but increase in pH at 9 showed only small decrease in the photodegradation efficiency.

As shown in figure (11) shows the initial rate of 4-NT photodegradation process in different solution pH, this results as similar to the results photodegradation of permethrin on TiO_2 surface was obtained in acidic medium (pH7 and pH2) occurs the highest rate of photodegradation [19].

The surface of titanium dioxide can be protonated or deprotonated under acidic or alkaline conditions, according to the following reactions.

$$TiOH + H^+ \; TiOH_2^+ \quad (4)$$

$$TIOH + OH^- \; TiO- + H_2O \quad (5)$$

Titania surface will remain positively charged in acidic medium and negatively charged in alkaline medium [20].

3.4. Effect of Temperature on Photodegradation of 4-NT by TiO_2/CdS Nanoparticle

The dependence of photocatalytic activity with temperature [21] generally the increase in temperature enhances recombination of charge carriers, resulting in a decrease of photocatalytic activity [15].

The photodegradation reaction for 4- NT have been carried out by varying the reaction temperature from 288 to 318 k figure (12) shows represent the rate constant for 4-NT in aqueous TiO_2 /CdS suspension at different temperatures at 298 k occurs higher degradation efficiency (75.26%).

Figure (13) shows Arrhenius plot of the reaction rate constant versus reciprocal of temperature, from the slope of the straight line obtained the activation energy equal to (1.3055 KJ/ mol), is generally temperature independent. Most reduce the nanoparticle activity of TiO_2/CdS when the reaction temperature rises.

Hofstadler and Coworkers [22] found the activation energy of photocatalytic degradation of 4- chlorophenol on TiO_2 surface is equal to 6.4 KJ/mol and 20.6 KJ/mol.

3.5. Effect Different of Sources Light

The rate of photodegradation of 4-NT in aqueous TiO_2 coupled CdS suspension determined under (UV-light, visible light and sun light) irradiation.

The result observed in figure (14) and figure (15) shows the degradation efficiency (83.04%) under 300 watt.

Ions S^{-2} in CdS is easily oxidized by photogenerated hols, which is accompanied by the release of Cd^{2+} into solution. that the efficiency of material doped TiO_2 under visible light depended on the preparation method used.

In same cases such doped photocatalysts showed lower activity in the UV-light. [23]

The optical condition of TiO_2 coupled CdS nanoparticle (0.125 g/l) of photodegradation of P-NT of concentration ($7*10^{-4}$M) for P-NT, pH 7, T 25°C and visible –light.

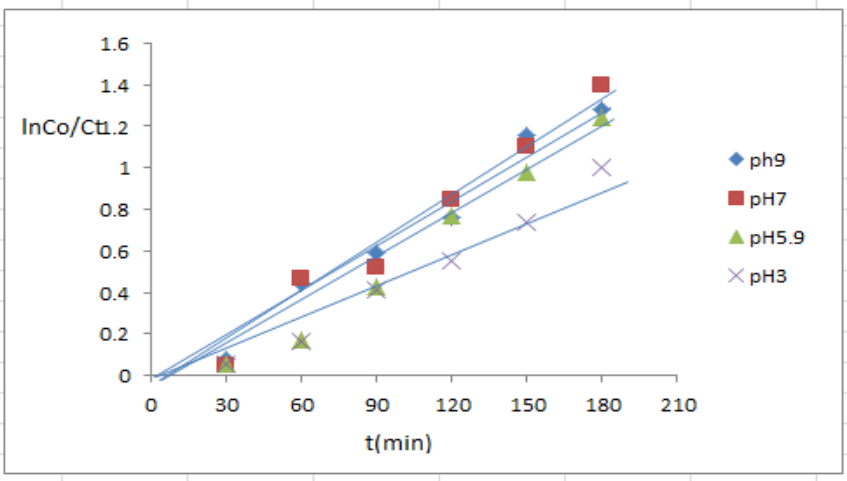

Figure (11). pH different of nanoparticle TiO_2/CdS (0.125 g/l), 4-NT($7*10^{-4}$)M

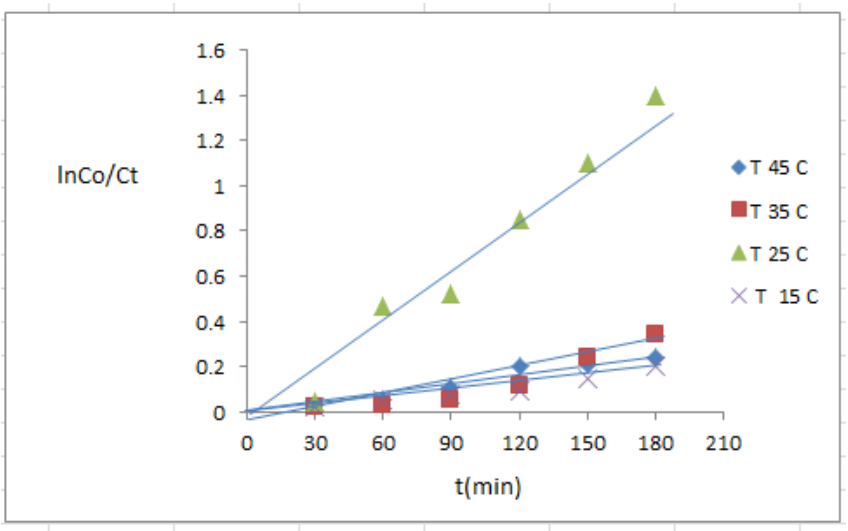

Figure (12). Temperature different of nanoparticleTiO_2/ CdS (0.125 g/l), 4-NT($7*10^{-4}$)M, pH7

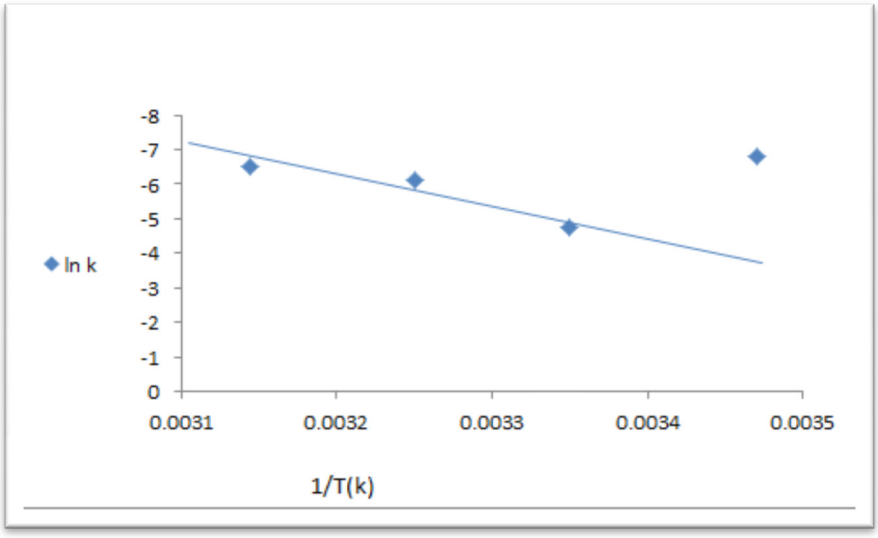

Figure (13). Arrhenius plot for the degradation of p-N.T ($7*10^{-4}$M) on irradiated TiO_2/CdS nanopartical (0.125 g/l)

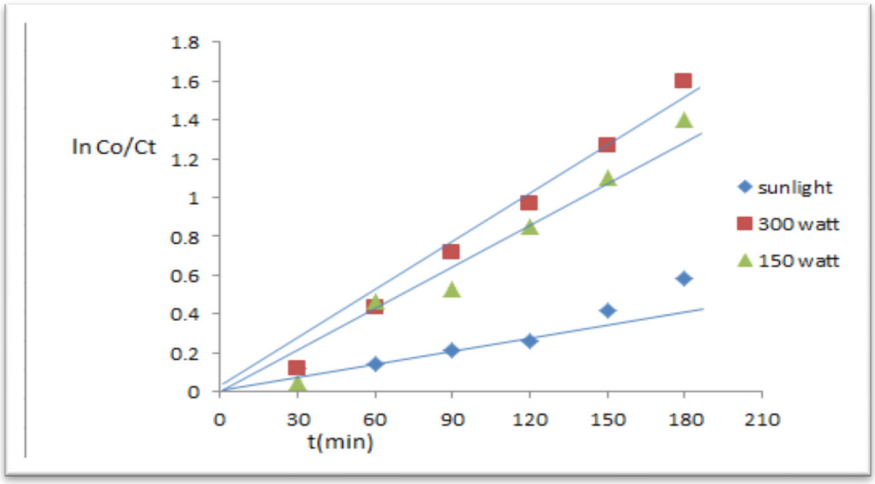

Figure (14). Sources different of nanoparticle TiO_2/CdS (0.125 g/l), 4-NT($7*10^{-4}$)M, pH7

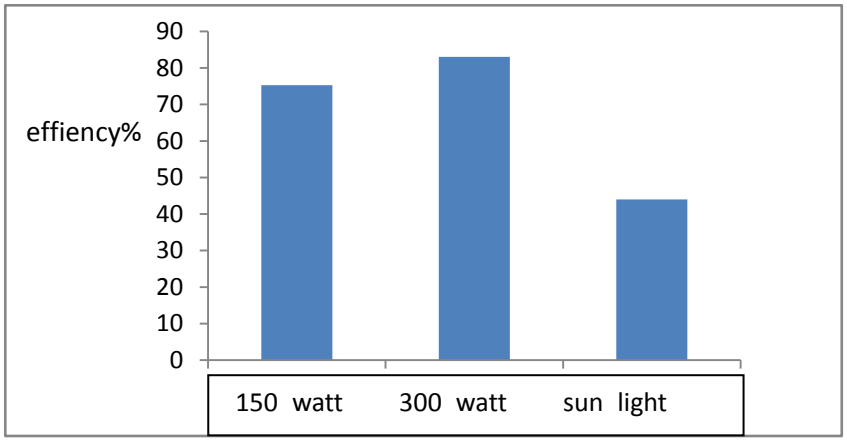

Figure (15). Effiency of sources light of degradation 4-NT

4. Conclusions

In this work TiO_2/CdS photocatalyst was prepared by sol-gel method and its photocatalytic activity on degradation of organic material were tested, coupling with CdS could narrow the band gap of TiO_2 and the absorption to visible –light region. Particle size of TiO_2/CdS (42) nm, Surface area of TiO_2/CdS was (18.69) m^2g^{-1} with average pore diameter (132.7) A^o.

The photodegradation study of p-nitrotolune provides for highly efficiency method degradation of P-nitrotolune was degraded within 180 min when 0.125 $gm.l^{-1}$ of TiO_2/CdS nanoparticle at pH 7 under 300 watt that photocatalyst degraded products were less toxic.

REFERENCES

[1] J. Carlos Colmenares, Rluque, J Manuel Campelo, F. Colmenares, Z Karpiński and A. Angel Romero (Nanostructured Photocatalysts and Their Applications in the Photocatalytic Transformation of Lignocellulosic Biomass: An Overview) Materials, *2*, 2228-2258, 2009.

[2] L. Qi, H. Colfen, M. Antonietti (synthesis and characterization of CdS nanoparticles stabilized by double – Hydrophilicblock copolymers) Nanoletters, Vol.1, No.2, 61-65, 2001.

[3] G. A. Martinez-Gastanon, M. G. San Chez- Lovedo, J.R. Martinez - Mendoza and Facundo Ruiz. (Synthsis of Cds nanoparticles: a simple method in Aqueous media) vol.1, 2005.

[4] S. S. Kumar, P. V. Swarlu, V. R. Rao, G.N. Rao (Synthesis, Charaterization and optical properties of zinc oxide nanoparticles) International Nano Letters, 1-6, 3:30, 2013.

[5] R. Nainani, P. Thakur, M. Chaskar (Synthesis of siliver doped TiO_2 nanoparticles for the improved photocatalytic degradation of methyl orange) Journal of materials science and engineering B2(1), 52-58, 2012.

[6] Y. F. Chen, C. Y. Lee, M.Y. Tang, H.T. Chiu (The effect of calcinations temperature on the crystallinite of TiO_2 nanopowders) Journal of crystal Growth .247, 363-370, 2003.

[7] K. Thangavelu, R. Annamalai, D. Arulnandhi (Preparation and characterization of Nanosized TiO_2 powder by sol- gel precipitation route) International journal of emerging Technology and advanced Engineering. Vol 3, 636-640, 2013.

[8] R. Vijayalakshmi, V. Rajendran (Synthesis and characterization of nano-TiO_2 via different methods) Archives of applied science research, 4(2), 1183-1190, 2012.

[9] Warren B.E (X-ray diffraction) Dover, New York 1990.

[10] Y. Badr, M. A. Mahmoud, (Size-dependent spectroscopic, optical, and electrical properties of PbSe nanoparticles) Cryst. Res. Technol. 41, 658-663, 2006.

[11] J. Barman, J. P. Borah, K. C. Sarma (Synthesis and characterization of CdSnano particles by chemical growth technique) Optoelectronics and advanced materials rapid communications, Vol 2, No.12, 770-774,2008.

[12] A. Tumuluir, K. Lakshun Naidu, K.C. James Raju. (Band gap determination using Taucs plot for $LiNbO_3$ thin films) International Journal of Chem Tech Research, 6(6), 3353-3356, 2014.

[13] F. Sayilkan, M. Asilturk, H. Sayilkan, Y. Onal, M. Akarsu, E. Arpag (Characterization of TiO_2 synthesized in alcohol by a sol-gel process: The effects of annealing temperature and acid catalyst) Turk. J. Chem.29, 697-706, 2005.

[14] E. Kraleva, H. Ehrich (Synthesis characterization and activity of Co and Ni catalysts supported on AlMe (Me = Zn, Zr, Ti) mixed oxides) J.Sol- Gel Sci Technol 64, 619-626, 2012.

[15] J.C. Colmenares, M.A. Aramendía, A. Marinas, J.M. Marinas, F.J. Urbano, Synthesis, characterisation and photocatalytic activity of different metal doped titania systems. Appl. Catal. A, 306, 120–127, 2006.

[16] M. M. Ba-Abbad, A. A. Kadhum, A. B. Mohamad, M. S. Takriff (Synthesis and catalytic activity of TiO_2 Nanoparticles for photochemical oxidation of concentrated chlorophenols under direct solar radiation) Int.J. Electrochem. Sci, 7, 4871-4888, 2012.

[17] D. M. Fouad, M. B. Mohamed (Coparative study of the photocatalytic activity of semiconductor Nanostructures and their hybrid metal Nanocomposites on the photodegradation of malathion) Journal of Nanomaterials, Vol.2012, 1-8, 2011.

[18] P. V. Kamat, R. Huehn, R. Nicolaescn (A sense and shoot

approach forphotocatalytic degradation of organic contaminants in water) Journal of physical chemistry B, Vol. 96, No.4, 788-794, 2007.

[19] H. Hidaka, K. Nohara, J. Zhao, (photooxidative degradation of pesiticide permethrin catalyzed by TiO_2 semiconductor slurries in aqueous media) J. photochem.photobiolo:A:chem . 64, 247-254, 1992.

[20] J. Sun, X. Wang, J. Sun,; Sun, R. Sun, S.; Qiao, L. Photocatalytic degradation and kinetics of Orange G using nano-sized Sn(IV)/TiO_2/AC photocatalyst. J. Mol. Catal. A., 260,241–246, 2006.

[21] E. T. Soares, M.A. Lansarin, C. C. Moro (A study of process variables for the photocatalytic degradation of rhodamine B. Brazilian) J. Chem. Eng. 24, 29–36, 2007.

[22] K. Hofstadler, G. Rupper, R. Bauer, G. Heisler, S. Novalic (Photocatalyic purification of water and air) D.F.Ollis and H.AL-Ekabi (Eds). Elsevier, N. Y, 777-782, 1993.

[23] A. Zaleska (Doped-TiO_2: A Review) Recent Patents on Engineering 2, 157-164, 2008.